MATCH
Communications in Mathematical and in Computer Chemistry

MATCH Commun. Math. Comput. Chem. **89** (2023) 529–566
ISSN: 0340–6253
doi: 10.46793/match.89-3.529M

Further Insight Into Bifurcation and Hybrid Control Tactics of a Chlorine Dioxide–Iodine–Malonic Acid Chemical Reaction Model Incorporating Delays

Dan Mu[a], Changjin Xu[b,*], Zixin Liu[a], Yicheng Pang[a]

[a] *School of Mathematics and Statistics, Guizhou University of Finance and Economics, Guiyang 550025, PR China*

[b] *Guizhou Key Laboratory of Economics System Simulation, Guizhou University of Finance and Economics, Guiyang 550025, PR China*

xcj403@126.com, md980929@126.com, xinxin905@126.com, ypanggy@outlook.com

(Received October 28, 2022)

Abstract

Delayed differential equation is an important tool to describe the interaction of different chemical substance in chemistry. In this present research, we set up a novel chlorine dioxide-iodine-malonic acid chemical reaction model incorporating delays. The peculiarity of solution and Hopf bifurcation of the formulated delayed chlorine dioxide-iodine-malonic acid chemical reaction model are explored. Firstly, the existence and uniqueness is investigated via fixed point theorem. Secondly, the non-negativeness of solution is studied via some proper mathematical inequality shills. Thirdly, the stability and bifurcation of the formulated delayed chlorine dioxide-iodine-malonic acid chemical reaction model are analyzed. The influence of delay on the delayed chlorine dioxide-iodine-malonic acid chemical reaction model is uncovered. Fourthly, Hopf bifurcation control issue of the formulated delayed chlorine dioxide-iodine-malonic acid chemical reaction model is studied via two hybrid controllers. To

*Corresponding author.

check the soundness of acquired key assertions, Matlab simulations are executed. The gained assertions of this research are completely novel and possess tremendous theoretical value in maintaining the balance of the concentrations of chlorine dioxide, iodine in chemistry.

1 Introduction

Usually, the interaction of different chemical substance displays very complex dynamical phenomenon in natural world. The Belousov-Zhabotinsky reaction (BZ reaction), which first proposed by Belousov [1] and Zhabotinskii [2], represents the classical chemical reaction of non-equilibrium thermodynamics. It can generate chemical periodic oscillation phenomenon [3]. The chemical periodic oscillation phenomenon often quite complicated. Generally speaking, the BZ reaction comprises more than twenty chemical reaction procedures, but it can be boiled down to three differential equations [3]. In 1990, Lengyel et al. [4] explored the chemical oscillations of the chlorine dioxide-iodine-malonic acid reaction($\mathcal{C}l\mathcal{O}_2 - \mathcal{I}_2 - \mathcal{MA}$). The tree chemical reactions are represented as follows:
(i) The iodination reaction of malonic acid ($\mathcal{MA}$) obeys the following rule:

$$\mathcal{MA} + \mathcal{I}_2 \rightarrow \mathcal{IMA} + \mathcal{I}^- + \mathcal{H}^+. \tag{1}$$

(ii)The oxidation reaction for iodide ions from free chlorine dioxide radical obeys the following rule:

$$\mathcal{C}l\mathcal{O}_2 + \mathcal{I}^- \rightarrow \mathcal{C}l\mathcal{O}_2^- + \frac{1}{2}\mathcal{I}_2^2. \tag{2}$$

(iii)A reaction process between chlorite and iodide ions from the above two steps to produce iodine obeys the following rule:

$$\mathcal{C}l\mathcal{O}_2 + 4\mathcal{I}^- + 4\mathcal{H}^+ \rightarrow \mathcal{C}l + 2\mathcal{I}_2^2 + 2\mathcal{H}_2\mathcal{O}. \tag{3}$$

Then the chlorine dioxide-iodine-malonic acid($\mathcal{C}l\mathcal{O}_2 - \mathcal{I}_2 - \mathcal{MA}$) model can be expressed as follows:

$$\begin{cases} -\dfrac{d[\mathcal{I}_2]}{ds} = \dfrac{\kappa_{1\alpha}[\mathcal{MA}][\mathcal{I}_2]}{\kappa_{1\beta} + [\mathcal{I}_2]}, \\ -\dfrac{d[\mathcal{C}l\mathcal{O}_2]}{ds} = \kappa_2[\mathcal{C}l\mathcal{O}_2][\mathcal{I}^-], \\ -\dfrac{d[\mathcal{C}l\mathcal{O}_2^-]}{ds} = \kappa_{3\alpha}[\mathcal{C}l\mathcal{O}_2][\mathcal{I}^-][\mathcal{H}^+] + \kappa_{3\beta}[\mathcal{C}l\mathcal{O}_2][\mathcal{I}^-][\mathcal{I}_2]\dfrac{\mathcal{I}^-}{v + [\mathcal{I}^{-2}]}, \end{cases} \tag{4}$$

where $\kappa_{1\alpha}, \kappa_2, \kappa_{3\alpha}, \kappa_{3\beta}$ represent reaction rate constants, $\kappa_{1\beta}$ and v depict saturation phenomena;
$\kappa_{3\beta}[\mathcal{C}l\mathcal{O}_2][\mathcal{I}^-][\mathcal{I}_2]\frac{\mathcal{I}^-}{v+[\mathcal{I}^{-2}]}$ stands for the autocatalytic effect of $\mathcal{I}_2$ and the self-inhibitory effect of $\mathcal{I}^-$ on the chlorite-iodide reaction [3,5]. Experiment shows that concentrations of iodide and chlorite ions change quickly and the concentrations of malonic acid, chlorine dioxide and iodine change tardily. Thus we argue that the dynamical behavior of model (4) can be approximate to a model with merely two variables: the concentrations of iodide and chlorite ions. In a flow chemical reactor, remaining the concentrations of chlorine dioxide, iodine and malonic acid as constants, then $\mathcal{MA}, \mathcal{I}_2$ and $\mathcal{C}l\mathcal{O}_2$ change much more tardily than $\mathcal{I}^-$ and $\mathcal{C}l\mathcal{O}_2^-$. Let $\mathcal{X} = \mathcal{I}^-, \mathcal{Y} = \mathcal{C}l\mathcal{O}_2^-$, $\mathcal{A} = \mathcal{I}_2$, then we derive the equations as follows:

$$\begin{cases} \mathcal{A} \to \mathcal{X}, r_{\mathcal{M}_1} = \kappa_1^{'}, \kappa_1^{'} = \kappa_1[\mathcal{MA}]_0, \\ \mathcal{X} \to \mathcal{Y}, r_{\mathcal{M}_2} = \kappa_2^{'}[\mathcal{X}], \kappa_2^{'} = \kappa_2[\mathcal{C}l\mathcal{O}_2], \\ 4\mathcal{X} + \mathcal{Y} \to \mathcal{Y} \to \mathcal{P}, r_{\mathcal{M}_3} = \dfrac{\kappa_3^{'}[\mathcal{X}][\mathcal{Y}]}{v + [\mathcal{X}]^2}, \kappa_3^{'} = \kappa_{3\beta}[\mathcal{I}]_0. \end{cases} \tag{5}$$

Make variable substitutions: $\mathcal{X} = \alpha u_1, \mathcal{Y} = \beta u_2, s = \gamma t, \alpha = \sqrt{v}, \beta = \frac{v\kappa_2^{'}}{\kappa_3^{'}}, \gamma = \frac{1}{\kappa_2^{'}}, a = \frac{\gamma\kappa_1^{'}}{\alpha}, b = \frac{\alpha}{\beta}$, then we gain the 2D model as follows:

$$\begin{cases} \dfrac{du_1(t)}{dt} = a - u_1(t) - \dfrac{4u_1(t)u_2(t)}{1 + u_1^2(t)}, \\ \dfrac{du_2(t)}{dt} = bu_1(t)\left[1 - \dfrac{u_2(t)}{1 + u_1^2(t)}\right], \end{cases} \tag{6}$$

where u_1 and u_2 denote concentrations (in dimensionless forms) of $\mathcal{I}^-$ and $\mathcal{C}l\mathcal{O}_2^-$, respectively, a, b stand for kinetic coefficients. In 2018, Din et al. [3] carried out detailed analysis on the stability, Neimark-Sacker bifurcations of the discrete-time version of model (5). Notice that there is a delay of feedback response of the concentration of $\mathcal{I}^-$ in chemical reaction, we modify model (5) as the following delayed form:

$$\begin{cases} \dfrac{du_1(t)}{dt} = a - u_1(t-\rho) - \dfrac{4u_1(t)u_2(t)}{1+u_1^2(t)}, \\ \dfrac{du_2(t)}{dt} = bu_1(t)\left[1 - \dfrac{u_2(t)}{1+u_1^2(t)}\right], \end{cases} \tag{7}$$

where $\rho > 0$ is a time delay.

Hopf bifurcation driven by delay is an significant dynamical peculiarity in nonlinear delayed differential models [6–16]. In chemistry, Hopf bifurcation driven by delay can availably characterize the transformation relationship of the concentration of different chemical substances. Therefore we argue that it is of much concern to explore the Hopf bifurcation driven by delay in various chemical reaction models. Inspired by this analysis above, we are going to investigate the Hopf bifurcation driven by delay and the control issue of Hopf bifurcation for system (7). Specifically, we are to deal with the following aspects: **(a)** Seek the existence and uniqueness, non-negativeness of the solution of system (b). **(c)** explore the stability trait and the existence Hopf bifurcation of system (7). **(d)**control Hopf bifurcation of system (7) via two hybrid controllers.

The key contributions of this research are listed as follows: **(a)** Depending on the earlier literatures, we set up a novel chlorine dioxide-iodine-malonic acid chemical reaction model incorporating delays. **(b)** The sufficient criterion to ensure the stability and the generation of Hopf bifurcation of system (7) is gained. **(c)** By virtue of hybrid controllers, the stability region and the time of the generation of Hopf bifurcation of system (7) are successfully dominated. **(d)** The impact of delay on the stability and the generation of Hopf bifurcation of system (7) has been explored. **(e)** The control technique can be applied to investigate the Hopf bifurcation control aspect of lots of integer-order differential system in various subjects.

This research is arranged as follows. The existence and uniqueness, non-negativeness of the solution of system (7) are investigated in Segment 2. The stability trait and the generation of Hopf bifurcation of system (7) are analyzed in Segment 3. The Hopf bifurcation control problem of system (7) by virtue of a suitable hybrid controller that includes state feedback and parameter perturbation with delay is handled in Segment 4. The Hopf bifurcation control problem of system (7) by virtue of a suitable hybrid controller that includes state feedback and parameter perturbation without delay is handled in Segment 5. Segment 6 executes Matlab simulations to check the rationality of the gained results. Segment 7 finishes the research.

2 Peculiarity of the solution

In this segment, we are about to seek the existence and uniqueness, non-negativeness of the solution of system (7) by virtue of fixed point theorem and inequality skills.

Theorem 2.1. *Denote* $\Delta = \{u_1, u_2) \in R^2 : \max\{|u_1|, |u_2||\} \leq \mathcal{U}\}$, *where* $\mathcal{U} > 0$ *stands for a constant. For each* $(u_{10}, u_{20}) \in \Delta$, *system (7) concerning the initial condition* (u_{10}, u_{20}) *admits a unique solution* $U = (u_1, u_2) \in \Delta$.

Proof Define a mapping as follows:

$$f(U) = (f_1(U), f_2(U)), \tag{8}$$

where

$$\begin{cases} f_1(U) = a - u_1(t-\rho) - \dfrac{4u_1(t)u_2(t)}{1+u_1^2(t)}, \\ f_2(U) = bu_1(t)\left[1 - \dfrac{u_2(t)}{1+u_1^2(t)}\right]. \end{cases} \tag{9}$$

For arbitrary $U, \tilde{U} \in \Delta$, we gain

$$\begin{aligned} &||f(U) - f(\tilde{U})|| \\ &= \left| a - u_1(t-\rho) - \frac{4u_1(t)u_2(t)}{1+u_1^2(t)} - [a - \tilde{u}_1(t-\rho) - \frac{4\tilde{u}_1(t)\tilde{u}_2(t)}{1+\tilde{u}_1^2(t)}] \right| \end{aligned}$$

$$
\begin{aligned}
&+\left|bu_1(t)\left[1-\frac{u_2(t)}{1+u_1^2(t)}\right]-\left\{b\tilde{u}_1(t)\left[1-\frac{\tilde{u}_2(t)}{1+\tilde{u}_1^2(t)}\right]\right\}\right| \\
&\leq |u_1(t-\rho)-\tilde{u}_1(t-\rho)|+\frac{4}{(1+\mathcal{U}^2)^2}[\mathcal{U}|u_2(t)-\tilde{u}_2(t)| \\
&\quad +\mathcal{U}|u_1(t)-\tilde{u}_1(t)|+3\mathcal{U}^3|u_1(t)-\tilde{u}_1(t)| \\
&\quad +\mathcal{U}^3|u_2(t)-\tilde{u}_2(t)|]+b|u_1(t)-\tilde{u}_1(t)| \\
&\quad +\frac{1}{(1+\mathcal{U}^2)^2}[|u_2(t)-\tilde{u}_2(t)|+\mathcal{U}^2|u_2(t)-\tilde{u}_2(t)| \\
&\quad +2\mathcal{U}^3|u_1(t)-\tilde{u}_1(t)|] \\
&\quad \leq \left[1+b+\frac{4\mathcal{U}+14\mathcal{U}^3}{\mathcal{U}^2)^2}\right]|u_1(t)-\tilde{u}_1(t)| \\
&\quad +\left[\frac{1+4\mathcal{U}+\mathcal{U}^2+4\mathcal{U}^3}{\mathcal{U}^2)^2}\right]|u_2(t)-\tilde{u}_2(t)| \\
&\leq \vartheta||U-\tilde{U}||, \qquad (10)
\end{aligned}
$$

where

$$
\vartheta=\max\left\{1+b+\frac{4\mathcal{U}+14\mathcal{U}^3}{\mathcal{U}^2)^2},\frac{1+4\mathcal{U}+\mathcal{U}^2+4\mathcal{U}^3}{\mathcal{U}^2)^2}\right\}. \qquad (11)
$$

So $f(U)$ conforms to Lipschitz condition for U (see [17]). In view of fixed point theorem, one can lightly understand that Theorem 2.1 is correct. ■

Theorem 2.2. *If $\rho=0$, then all solutions to system (7) starting with R_+^2 are non-negative.*

Proof Assume that $U(t_0)=(u_1(t_0),u_2(t_0))$ is the initial value of system (7). Assume that there exists a positive constant $t_\star$ satisfying $t_0<t<t_\star$ obeying

$$
\begin{cases}
u_1(t)=0, t_0<t<t_\star, \\
u_1(t_\star)=0, \\
u_1(t_\star^+)<0.
\end{cases} \qquad (12)
$$

In view of system (7), one gets

$$
\frac{du_1(t)}{dt}|_{u_1(t_\star)=0}=a. \qquad (13)
$$

In view of Lemma 1 of Das et al. [18], one gains $u_1(t_\star^+) = 0$, which is a contradiction (see (12)). So $u_1(t) \geq 0$ for $t \geq t_0$. Similarly, we can lightly gain that $u_2(t) \geq 0$ for $t \geq t_0$. ■

3 Bifurcation research

It is easy to derive that system (7) has the following unique positive equilibrium point: $E(u_{1\star}, u_{2\star})$, where where

$$\begin{cases} u_{1\star} = \dfrac{a}{5}, \\ u_{2\star} = a + \dfrac{a^2}{25}. \end{cases} \tag{14}$$

The linear system of system (7) around $E(u_{1\star}, u_{2\star})$ takes the following expression:

$$\begin{cases} \dfrac{du_1(t)}{dt} = \left[\dfrac{8u_{1\star}^2 u_{2\star}}{(1+u_{1\star}^2)^2} - \dfrac{4u_{2\star}}{1+u_{1\star}^2}\right] u_1(t) - \dfrac{4u_{1\star}}{1+u_{1\star}^2} u_2(t) - u_1(t-\rho), \\ \dfrac{du_2(t)}{dt} = \left[b + \dfrac{2bu_{1\star}^2 u_{2\star}}{(1+u_{1\star}^2)^2}\right] u_1(t) - \dfrac{bu_{1\star}}{1+u_{1\star}^2} u_2(t). \end{cases} \tag{15}$$

The characteristic equation of system (15) owns the following expression:

$$\det \begin{bmatrix} \lambda - \left(\frac{8u_{1\star}^2 u_{2\star}}{(1+u_{1\star}^2)^2} - \frac{4u_{2\star}}{1+u_{1\star}^2}\right) + e^{-\lambda\rho} & \frac{4u_{1\star}}{1+u_{1\star}^2} \\ -\left(b + \frac{2bu_{1\star}^2 u_{2\star}}{(1+u_{1\star}^2)^2}\right) & \lambda + \frac{bu_{1\star}}{1+u_{1\star}^2} \end{bmatrix} = 0, \tag{16}$$

which leads to

$$\lambda^2 + a_1\lambda + a_2 + (\lambda + a_3)e^{-\lambda\rho} = 0, \tag{17}$$

where

$$\begin{cases} a_1 = \dfrac{4u_{2\star}}{1+u_{1\star}^2} - \dfrac{8u_{1\star}^2 u_{2\star}}{(1+u_{1\star}^2)^2} + \dfrac{bu_{1\star}}{1+u_{1\star}^2}, \\ a_2 = \dfrac{4bu_{1\star}u_{2\star}}{(1+u_{1\star}^2)^2} + \dfrac{4bu_{1\star}}{1+u_{1\star}^2}, \\ a_3 = \dfrac{bu_{1\star}}{1+u_{1\star}^2}. \end{cases} \tag{18}$$

If $\rho = 0$, then Eq.(17) reads as:

$$\lambda^2 + (a_1 + 1)\lambda + a_2 + a_3 = 0, \tag{19}$$

If

$$(\mathcal{G}_1)\ a_1 + 1 > 0, a_2 + a_3 > 0$$

is fulfilled, then the two roots λ_1, λ_2 of Eq. (19) have negative real parts. Thus the positive equilibrium point $E(u_{1\star}, u_{2\star})$ of model (7) involving $\rho = 0$ remains locally asymptotically stable level.

Suppose that $\lambda = i\phi$ is the root of Eq. (17). Then Eq.(17) takes

$$i\phi^2 + a_1 i\phi + a_2 + (i\phi + a_3)e^{-i\phi\rho} = 0, \tag{20}$$

which generates

$$-\phi^2 + ia_1\phi + a_2 + (i\phi + a_3)(\cos\phi\rho - i\sin\phi\rho) = 0. \tag{21}$$

It follows from (21) that

$$\begin{cases} a_3\cos\phi\rho + \phi\sin\phi\rho = \phi^2 - a_2, \\ \phi\cos\phi\rho - a_3\sin\phi\rho = -a_1\phi. \end{cases} \tag{22}$$

By (22), we have

$$a_3^2 + \phi^2 = (\phi^2 - a_2)^2 + (-a_1\phi)^2, \tag{23}$$

which means

$$\phi^4 + (a_1^2 - 2a_2 - 1)\phi^2 + a_2^2 - a_3^2 = 0. \tag{24}$$

Let

$$\Delta_1(\phi) = \phi^4 + (a_1^2 - 2a_2 - 1)\phi^2 + a_2^2 - a_3^2. \tag{25}$$

Suppose that

$$(\mathcal{G}_2)\ |a_2| < |a_3|$$

holds, noticing that $\lim_{\phi\to+\infty}\Delta_1(\phi) = +\infty > 0$, then we understand that Eq. (24) has at least one positive real root. Thus Eq. (17) has at least

one pair of purely roots. Without loss of generality, here we suppose that Eq. (24) admits four positive real roots (say $\phi_i, i = 1, 2, 3, 4$). According to (22), we have

$$\rho_i^{(k)} = \frac{1}{\phi_i}\left[\arccos\left(\frac{(a_3 - a_1)\phi_i^2 - a_2 a_3)}{\phi_i^2 + a_3^2}\right) + 2k\pi\right], \tag{26}$$

where $i = 1, 2, 3, 4; k = 0, 1, 2, \ldots$. Denote

$$\rho_0 = \min_{\{i=1,2,3,4;k=0,1,2,\cdots\}}\{\rho_i^{(k)}\},$$

and suppose that when $\rho = \rho_0$, (17) admits a pair of imaginary roots $\pm i\phi_0$. Next the following assumption is needed:

$$(\mathcal{G}_3)\quad \mathcal{H}_{1R}\mathcal{H}_{2R} + \mathcal{H}_{1I}\mathcal{H}_{2I} > 0,$$

where

$$\begin{cases} \mathcal{H}_{1R} = a_1 + \cos\phi_0\rho_0, \\ \mathcal{H}_{1I} = 2\phi_0 - \sin\phi_0\rho_0, \\ \mathcal{H}_{2R} = a_3\sin\phi_0\rho_0 - \phi_0^2\cos\phi_0\rho_0, \\ \mathcal{H}_{2I} = \phi_0^2\sin\phi_0\rho_0 + a_3\phi_0\cos\phi_0\rho_0. \end{cases} \tag{27}$$

Lemma 3.1. *Denote $\lambda(\rho) = \epsilon_1(\rho) + i\epsilon_2(\rho)$ the root of Eq. (17) near $\rho = \rho_0$ such that $\epsilon_1(\rho_0) = 0, \epsilon_2(\rho_0) = \phi_0$, then $Re\left(\frac{d\lambda}{d\rho}\right)\Big|_{\rho=\rho_0,\phi=\phi_0} > 0$.*

Proof Using Eq.(17), we gain

$$2\lambda\frac{d\lambda}{d\rho} + a_1\frac{d\lambda}{d\rho} + \frac{d\lambda}{d\rho}e^{-\lambda\rho} - \frac{d\lambda}{d\rho}\left(\lambda + \rho\frac{d\lambda}{d\rho}\right)(\lambda + a_3)e^{-\lambda\rho} = 0, \tag{28}$$

which implies

$$\left(\frac{d\lambda}{d\rho}\right)^{-1} = \frac{\mathcal{H}_1(\lambda)}{\mathcal{H}_2(\lambda)} - \frac{\rho}{\lambda}, \tag{29}$$

where

$$\begin{cases} \mathcal{H}_1(\lambda) = 2\lambda + a_1 + e^{-\lambda\rho}, \\ \mathcal{H}_2(\lambda) = \lambda(\lambda + a_3)e^{-\lambda\rho}. \end{cases} \tag{30}$$

Hence

$$\mathrm{Re}\left[\left(\frac{d\lambda}{d\rho}\right)^{-1}\right]_{\rho=\rho_0,\phi=\phi_0} = \mathrm{Re}\left[\frac{\mathcal{H}_1(\lambda)}{\mathcal{H}_2(\lambda)}\right]_{\rho=\rho_0,\phi=\phi_0} = \frac{\mathcal{H}_{1R}\mathcal{H}_{2R}+\mathcal{H}_{1I}\mathcal{H}_{2I}}{\mathcal{H}_{2R}^2+\mathcal{H}_{2I}^2}. \tag{31}$$

In view of $(\mathcal{G}_3)$, we gain

$$\mathrm{Re}\left[\left(\frac{d\lambda}{d\rho}\right)^{-1}\right]_{\rho=\rho_0,\phi=\phi_0} > 0, \tag{32}$$

which ends the proof. ■

Depending on the discussion above, the following outcomes is lightly gained.

Theorem 3.1. *Suppose that* $(\mathcal{G}_1)$-$(\mathcal{G}_3)$ *are true, then the positive equilibrium point* $E(u_{1\star}, u_{2\star})$ *of model (7) is locally asymptotically stable if* $\rho \in [0, \rho_0)$ *and model (7) generates a Hopf bifurcation around the positive equilibrium point* $E(u_{1\star}, u_{2\star})$ *when* $\rho = \rho_0$.

4 Bifurcation domination via hybrid controller I

In this part, we will deal with the Hopf bifurcation problem of system (7) via a suitable hybrid controller consisting of state feedback and parameter perturbation with delay. Taking advantage of the idea in [19, 20], we obtain the following controlled chlorine dioxide-iodine-malonic acid chemical reaction model:

$$\begin{cases} \dfrac{du_1(t)}{dt} = \varrho_1\left[a - u_1(t-\rho) - \dfrac{4u_1(t)u_2(t)}{1+u_1^2(t)}\right] + \varrho_2[u_1(t-\rho) - u_1(t)], \\ \dfrac{du_2(t)}{dt} = bu_1(t)\left[1 - \dfrac{u_2(t)}{1+u_1^2(t)}\right], \end{cases} \tag{33}$$

where ϱ_1, ϱ_2 stands for feedback gain parameters. System (33) and system (7) owns the same equilibrium points $E(u_{1\star}, u_{2\star})$. The linear system of

system (33) around $E(u_{1\star}, u_{2\star})$ takes the following expression:

$$\begin{cases} \dfrac{du_1(t)}{dt} = \left[\varrho_1\left(\dfrac{8u_{1\star}^2u_{2\star}}{(1+u_{1\star}^2)^2} - \dfrac{4u_{2\star}}{1+u_{1\star}^2}\right) - \varrho_2\right]u_1(t) \\ \qquad\qquad - \dfrac{4u_{1\star}\varrho_1}{1+u_{1\star}^2}u_2(t) + (\varrho_2-\varrho_1)u_1(t-\rho), \\ \dfrac{du_2(t)}{dt} = \left[b + \dfrac{2bu_{1\star}^2u_{2\star}}{(1+u_{1\star}^2)^2}\right]u_1(t) - \dfrac{bu_{1\star}}{1+u_{1\star}^2}u_2(t). \end{cases} \tag{34}$$

The characteristic equation of system (34) owns the following expression:

$$\det\begin{bmatrix} \lambda - \left[\varrho_1\left(\frac{8u_{1\star}^2u_{2\star}}{(1+u_{1\star}^2)^2} - \frac{4u_{2\star}}{1+u_{1\star}^2}\right) - \varrho_2\right] - (\varrho_2-\varrho_1)e^{-\lambda\rho} & \frac{4u_{1\star}\varrho_1}{1+u_{1\star}^2} \\ -\left(b + \frac{2bu_{1\star}^2u_{2\star}}{(1+u_{1\star}^2)^2}\right) & \lambda + \frac{bu_{1\star}}{1+u_{1\star}^2} \end{bmatrix} = 0, \tag{35}$$

which leads to

$$\lambda^2 + b_1\lambda + b_2 + (b_3\lambda + b_4)e^{-\lambda\rho} = 0, \tag{36}$$

where

$$\begin{cases} b_1 = \dfrac{bu_{1\star}}{1+u_{1\star}^2} - \left[\varrho_1\left(\dfrac{8u_{1\star}^2u_{2\star}}{(1+u_{1\star}^2)^2} - \dfrac{4u_{2\star}}{1+u_{1\star}^2}\right) - \varrho_2\right], \\ b_2 = -\left[\varrho_1\left(\dfrac{8u_{1\star}^2u_{2\star}}{(1+u_{1\star}^2)^2} - \dfrac{4u_{2\star}}{1+u_{1\star}^2}\right) - \varrho_2\right]\dfrac{bu_{1\star}}{1+u_{1\star}^2}, \\ b_3 = -(\varrho_2-\varrho_1), \\ b_4 = (\varrho_2-\varrho_1)\dfrac{bu_{1\star}}{1+u_{1\star}^2}. \end{cases} \tag{37}$$

If $\rho = 0$, then Eq.(36) reads as:

$$\lambda^2 + (b_1+b_3)\lambda + b_2 + b_4 = 0, \tag{38}$$

If

$$(\mathcal{G}_4)\ b_1 + b_3 > 0, b_2 + b_4 > 0$$

is fulfilled, then the two roots λ_1, λ_2 of Eq. (38) have negative real parts. Thus the positive equilibrium point $E(u_{1\star}, u_{2\star})$ of model (33) involving $\rho = 0$ remains locally asymptotically stable level.

Suppose that $\lambda = i\omega$ is the root of Eq. (36). Then Eq.(36) takes

$$(i\omega)^2 + b_1 i\omega + b_2 + (b_3 i\omega + b_4)e^{-i\omega\rho} = 0, \tag{39}$$

which generates

$$-\omega^2 + b_1 i\omega + b_2 + (b_3 i\omega + b_4)(\cos\omega\rho - i\sin\omega\rho) = 0. \tag{40}$$

It follows from (40) that

$$\begin{cases} b_4\cos\omega\rho + b_3\omega\sin\omega\rho = \omega^2 - b_2, \\ b_3\omega\cos\omega\rho - b_4\sin\omega\rho = -b_1\omega. \end{cases} \tag{41}$$

By (41), we have

$$b_4^2 + (b_3\omega)^2 = (\omega^2 - b_2)^2 + (-b_1\omega)^2, \tag{42}$$

which means

$$\omega^4 + (b_1^2 - 2b_2 - b_3^2)\omega^2 + b_2^2 - b_4^2 = 0. \tag{43}$$

Let

$$\Delta_2(\omega) = \omega^4 + (b_1^2 - 2b_2 - b_3^2)\omega^2 + b_2^2 - b_4^2. \tag{44}$$

Suppose that

$$(\mathcal{G}_5)\ |b_2| < |b_4|$$

holds, noticing that $\lim_{\omega\to+\infty}\Delta_2(\omega) = +\infty > 0$, then we understand that Eq. (43) has at least one positive real root. Thus Eq. (36) has at least one pair of purely roots. Without loss of generality, here we suppose that Eq. (43) admits four positive real roots (say $\omega_j, j = 1, 2, 3, 4$). According to (41), we have

$$\rho_j^{(h)} = \frac{1}{\omega_j}\left[\arccos\left(\frac{b_4(\omega_j^2 - b_2) - b_1 b_3\omega_j^2}{b_4^2 + b_3^2\omega_j^2}\right) + 2h\pi\right], \tag{45}$$

where $j = 1, 2, 3, 4; h = 0, 1, 2, \cdots$. Denote

$$\rho_{0\star} = \min_{\{j=1,2,3,4;h=0,1,2,\cdots\}} \{\rho_j^{(h)}\},$$

and suppose that when $\rho = \rho_{0\star}$, (36) admits a pair of imaginary roots $\pm i\omega_0$.

Next the following assumption is needed:

$$(\mathcal{G}_6) \quad \mathcal{S}_{1R}\mathcal{S}_{2R} + \mathcal{S}_{1I}\mathcal{S}_{2I} > 0,$$

where

$$\begin{cases} \mathcal{S}_{1R} = b_1 + b_3 \cos\omega_0\rho_{0\star}, \\ \mathcal{S}_{1I} = 2\omega_0 - b_3 \sin\omega_0\rho_{0\star}, \\ \mathcal{S}_{2R} = b_4\omega_0 \cos\omega_0\rho_{0\star} + b_1\omega_0^2 \sin\omega_0\rho_{0\star}, \\ \mathcal{S}_{2I} = b_1\omega_0^2 \cos\omega_0\rho_{0\star} - b_4\omega_0 \sin\omega_0\rho_{0\star}. \end{cases} \tag{46}$$

Lemma 4.1. *Denote $\lambda(\rho) = \zeta_1(\rho) + i\zeta_2(\rho)$ the root of Eq. (36) near $\rho = \rho_{0\star}$ such that $\zeta_1(\rho_{0\star}) = 0, \zeta_2(\rho_{0\star}) = \omega_0$, then $Re\left(\frac{d\lambda}{d\rho}\right)\Big|_{\rho=\rho_{0\star},\omega=\omega_0} > 0$.*

Proof Using Eq.(36), we gain

$$2\lambda\frac{d\lambda}{d\rho} + b_1\frac{d\lambda}{d\rho} + b_3\frac{d\lambda}{d\rho}e^{-\lambda\rho} - \frac{d\lambda}{d\rho}\left(\lambda + \rho\frac{d\lambda}{d\rho}\right)(b_3\lambda + b_4)e^{-\lambda\rho} = 0, \tag{47}$$

which implies

$$\left(\frac{d\lambda}{d\rho}\right)^{-1} = \frac{\mathcal{S}_1(\lambda)}{\mathcal{S}_2(\lambda)} - \frac{\rho}{\lambda}, \tag{48}$$

where

$$\begin{cases} \mathcal{S}_1(\lambda) = 2\lambda + b_1 + b_3e^{-\lambda\rho}, \\ \mathcal{S}_2(\lambda) = \lambda(b_3\lambda + b_4)e^{-\lambda\rho}. \end{cases} \tag{49}$$

Hence

$$\mathrm{Re}\left[\left(\frac{d\lambda}{d\rho}\right)^{-1}\right]_{\rho=\rho_0,\phi=\phi_0} = \mathrm{Re}\left[\frac{\mathcal{S}_1(\lambda)}{\mathcal{S}_2(\lambda)}\right]_{\rho=\rho_{0\star},\omega=\omega_0} = \frac{\mathcal{S}_{1R}\mathcal{S}_{2R} + \mathcal{S}_{1I}\mathcal{S}_{2I}}{\mathcal{S}_{2R}^2 + \mathcal{S}_{2I}^2}. \tag{50}$$

In view of $(\mathcal{G}_6)$, we gain

$$\mathrm{Re}\left[\left(\frac{d\lambda}{d\rho}\right)^{-1}\right]_{\rho=\rho_{0\star},\omega=\omega_0} > 0, \tag{51}$$

which ends the proof. ■

Depending on the discussion above, the following outcomes is lightly gained.

Theorem 4.1. *Suppose that* $(\mathcal{G}_4)$-$(\mathcal{G}_6)$ *are true, then the positive equilibrium point* $E(u_{1\star}, u_{2\star})$ *of model (33) is locally asymptotically stable if* $\rho \in [0, \rho_{0\star})$ *and model (33) generates a Hopf bifurcation around the positive equilibrium point* $E(u_{1\star}, u_{2\star})$ *when* $\rho = \rho_{0\star}$.

5 Bifurcation domination via hybrid controller II

In this part, we will deal with the Hopf bifurcation problem of system (7) via a suitable hybrid controller consisting of state feedback and parameter perturbation without delay. Taking advantage of the idea in [21], we obtain the following controlled chlorine dioxide-iodine-malonic acid chemical reaction model:

$$\begin{cases} \dfrac{du_1(t)}{dt} = (1-\varrho)\left[a - u_1(t-\rho) - \dfrac{4u_1(t)u_2(t)}{1+u_1^2(t)}\right] + \varrho[u_1(t) - u_{1\star}], \\ \dfrac{du_2(t)}{dt} = bu_1(t)\left[1 - \dfrac{u_2(t)}{1+u_1^2(t)}\right], \end{cases} \tag{52}$$

where ϱ stands for control parameter. System (52) and system (7) owns the same equilibrium points $E(u_{1\star}, u_{2\star})$. The linear system of system (52) around $E(u_{1\star}, u_{2\star})$ takes the following expression:

$$\begin{cases} \dfrac{du_1(t)}{dt} = \left[\varrho + (1-\varrho)\left(\dfrac{8u_{1\star}^2u_{2\star}}{(1+u_{1\star}^2)^2} - \dfrac{4u_{2\star}}{1+u_{1\star}^2}\right)\right]u_1(t) \\ \qquad\qquad - \dfrac{4u_{1\star}(1-\varrho)}{1+u_{1\star}^2}u_2(t) - (1-\varrho)u_1(t-\rho), \\ \dfrac{du_2(t)}{dt} = \left[b + \dfrac{2bu_{1\star}^2u_{2\star}}{(1+u_{1\star}^2)^2}\right]u_1(t) - \dfrac{bu_{1\star}}{1+u_{1\star}^2}u_2(t). \end{cases} \tag{53}$$

The characteristic equation of system (53) owns the following expression:

$$\det\begin{bmatrix} \lambda-\left[\varrho+(1-\varrho)\left(\frac{8u_{1\star}^2u_{2\star}}{(1+u_{1\star}^2)^2}-\frac{4u_{2\star}}{1+u_{1\star}^2}\right)\right]+(1-\varrho)e^{-\lambda\rho} & \frac{4u_{1\star}(1-\varrho)}{1+u_{1\star}^2} \\ -\left(b+\frac{2bu_{1\star}^2u_{2\star}}{(1+u_{1\star}^2)^2}\right) & \lambda+\frac{bu_{1\star}}{1+u_{1\star}^2} \end{bmatrix}=0, \tag{54}$$

which leads to

$$\lambda^2+d_1\lambda+d_2+(d_3\lambda+d_4)e^{-\lambda\rho}=0, \tag{55}$$

where

$$\begin{cases} d_1=\dfrac{bu_{1\star}}{1+u_{1\star}^2}-\left[\varrho+(1-\varrho)\left(\dfrac{8u_{1\star}^2u_{2\star}}{(1+u_{1\star}^2)^2}-\dfrac{4u_{2\star}}{1+u_{1\star}^2}\right)\right], \\ d_2=\dfrac{4u_{1\star}(1-\varrho)}{1+u_{1\star}^2}\left(b+\dfrac{2bu_{1\star}^2u_{2\star}}{(1+u_{1\star}^2)^2}\right) \\ \qquad -\dfrac{bu_{1\star}}{1+u_{1\star}^2}\left[\varrho+(1-\varrho)\left(\dfrac{8u_{1\star}^2u_{2\star}}{(1+u_{1\star}^2)^2}-\dfrac{4u_{2\star}}{1+u_{1\star}^2}\right)\right], \\ d_3=1-\varrho, \\ d_4=\dfrac{bu_{1\star}(1-\varrho)}{1+u_{1\star}^2}. \end{cases} \tag{56}$$

If $\rho=0$, then Eq.(55) reads as:

$$\lambda^2+(d_1+d_3)\lambda+d_2+d_4=0, \tag{57}$$

If

$$(\mathcal{G}_7)\ d_1+d_3>0, d_2+d_4>0$$

is fulfilled, then the two roots λ_1,λ_2 of Eq. (57) have negative real parts. Thus the positive equilibrium point $E(u_{1\star},u_{2\star})$ of model (52) involving $\rho=0$ remains locally asymptotically stable level.

Suppose that $\lambda=i\varpi$ is the root of Eq. (55). Then Eq.(55) takes

$$(i\varpi)^2+d_1i\varpi+b_2+(d_3i\varpi+d_4)e^{-i\varpi\rho}=0, \tag{58}$$

which generates

$$-\varpi^2+d_1i\varpi+d_2+(d_3i\varpi+d_4)(\cos\varpi\rho-i\sin\varpi\rho)=0. \tag{59}$$

It follows from (59) that

$$\begin{cases} d_4\cos\varpi\rho + d_3\varpi\sin\varpi\rho = \varpi^2 - d_2, \\ d_3\varpi\cos\varpi\rho - d_4\sin\varpi\rho = -d_1\varpi. \end{cases} \tag{60}$$

By (60), we have

$$d_4^2 + (d_3\varpi)^2 = (\varpi^2 - d_2)^2 + (-d_1\varpi)^2, \tag{61}$$

which means

$$\varpi^4 + (d_1^2 - 2d_2 - d_3^2)\varpi^2 + d_2^2 - d_4^2 = 0. \tag{62}$$

Let

$$\Delta_3(\varpi) = \varpi^4 + (d_1^2 - 2d_2 - d_3^2)\varpi^2 + d_2^2 - d_4^2. \tag{63}$$

Suppose that

$$(\mathcal{G}_8)\ |d_2| < |d_4|$$

holds, noticing that $\lim_{\varpi\to+\infty}\Delta_3(\varpi) = +\infty > 0$, then we understand that Eq. (62) has at least one positive real root. Thus Eq. (55) has at least one pair of purely roots. Without loss of generality, here we suppose that Eq. (62) admits four positive real roots (say $\varpi_h, h = 1, 2, 3, 4$). According to (60), we have

$$\rho_h^{(k)} = \frac{1}{\varpi_h}\left[\arccos\left(\frac{d_4(\varpi_h^2 - d_2) - h_1h_3\varpi_h^2}{d_4^2 + d_3^2\varpi_h^2}\right) + 2k\pi\right], \tag{64}$$

where $h = 1, 2, 3, 4; k = 0, 1, 2, \cdots$. Denote

$$\rho_{0\diamond} = \min_{\{h=1,2,3,4;k=0,1,2,\cdots\}}\{\rho_h^{(k)}\},$$

and suppose that when $\rho = \rho_{0\diamond}$, (55) admits a pair of imaginary roots $\pm i\varpi_0$.

Next the following assumption is needed:

$$(\mathcal{G}_9)\ \ \mathcal{W}_{1R}\mathcal{W}_{2R} + \mathcal{W}_{1I}\mathcal{W}_{2I} > 0,$$

where

$$\begin{cases} \mathcal{W}_{1R} = d_1 + d_3 \cos \varpi_0 \rho_{0\diamond}, \\ \mathcal{W}_{1I} = 2\varpi_0 - d_3 \sin \varpi_0 \rho_{0\diamond}, \\ \mathcal{W}_{2R} = d_4 \varpi_0 \cos \varpi_0 \rho_{0\diamond} + d_1 \varpi_0^2 \sin \varpi_0 \rho_{0\diamond}, \\ \mathcal{W}_{2I} = d_1 \varpi_0^2 \cos \varpi_0 \rho_{0\diamond} - d_4 \varpi_0 \sin \varpi_0 \rho_{0\diamond}. \end{cases} \tag{65}$$

Lemma 5.1. *Denote $\lambda(\rho) = \theta_1(\rho) + i\theta_2(\rho)$ the root of Eq. (55) near $\rho = \rho_{0\diamond}$ such that $\zeta_1(\rho_{0\diamond}) = 0, \zeta_2(\rho_{0\diamond}) = \varpi_0$, then $Re\left(\frac{d\lambda}{d\rho}\right)\Big|_{\rho=\rho_{0\diamond},\varpi=\varpi_0} > 0$.*

Proof Using Eq.(55), we gain

$$2\lambda \frac{d\lambda}{d\rho} + d_1 \frac{d\lambda}{d\rho} + d_3 \frac{d\lambda}{d\rho} e^{-\lambda\rho} - \frac{d\lambda}{d\rho}\left(\lambda + \rho \frac{d\lambda}{d\rho}\right)(d_3\lambda + d_4)e^{-\lambda\rho} = 0, \tag{66}$$

which implies

$$\left(\frac{d\lambda}{d\rho}\right)^{-1} = \frac{\mathcal{W}_1(\lambda)}{\mathcal{W}_2(\lambda)} - \frac{\rho}{\lambda}, \tag{67}$$

where

$$\begin{cases} \mathcal{W}_1(\lambda) = 2\lambda + d_1 + d_3 e^{-\lambda\rho}, \\ \mathcal{W}_2(\lambda) = \lambda(d_3\lambda + d_4)e^{-\lambda\rho}. \end{cases} \tag{68}$$

Hence

$$\mathrm{Re}\left[\left(\frac{d\lambda}{d\rho}\right)^{-1}\right]_{\rho=\rho_{0\diamond},\varpi=\varpi_0} = \mathrm{Re}\left[\frac{\mathcal{W}_1(\lambda)}{\mathcal{W}_2(\lambda)}\right]_{\rho=\rho_{0\diamond},\varpi=\varpi_0} = \frac{\mathcal{W}_{1R}\mathcal{W}_{2R} + \mathcal{W}_{1I}\mathcal{W}_{2I}}{\mathcal{W}_{2R}^2 + \mathcal{W}_{2I}^2}. \tag{69}$$

In view of $(\mathcal{G}_9)$, we gain

$$\mathrm{Re}\left[\left(\frac{d\lambda}{d\rho}\right)^{-1}\right]_{\rho=\rho_{0\diamond},\varpi=\varpi_0} > 0, \tag{70}$$

which ends the proof. ■

Depending on the discussion above, the following outcomes is lightly gained.

Theorem 5.1. *Suppose that $(\mathcal{G}_7)$-$(\mathcal{G}_9)$ are true, then the positive equilibrium point $E(u_{1\star}, u_{2\star})$ of model (52) is locally asymptotically stable if $\rho \in [0, \rho_{0\diamond})$ and model (52) generates a Hopf bifurcation around the positive equilibrium point $E(u_{1\star}, u_{2\star})$ when $\rho = \rho_{0\diamond}$.*

Remark 5.1. *In 2018, Din et al. [3] dealt with the stability, bifurca-*

tion and chaos control of a discrete chlorine dioxide-iodine-malonic acid reaction model. In this article, we propose a new chlorine dioxide-iodine-malonic acid chemical reaction model incorporating delays. We have investigated the existence and uniqueness, boundedness of the solution, Hopf bifurcation and Hopf bifurcation control aspect of the formulated the delayed chlorine dioxide-iodine-malonic acid chemical reaction model (7). The exploration way of this article is different from that of Din et al. [3] and the acquired outcomes are completely new. Relying on this aspect, we argue that our works supplement the study of [4] to some degree.

6 Matlab simulations

Example 6.1. Consider the following chlorine dioxide-iodine-malonic acid chemical reaction model incorporating delays:

$$\begin{cases} \dfrac{du_1(t)}{dt} = 25 - u_1(t) - \dfrac{4u_1(t)u_2(t)}{1+u_1^2(t-\rho)}, \\ \dfrac{du_2(t)}{dt} = 10u_1(t)\left[1 - \dfrac{u_2(t)}{1+u_1^2(t-\rho)}\right]. \end{cases} \tag{71}$$

Obviously, system (71) owns a unique positive equilibrium point $E(5, 26)$. We can lightly check that the assumptions $(\mathcal{G}_1)$-$(\mathcal{G}_3)$ of Theorem 3.1 are satisfied. Taking advantage of Matlab software, we can gain that $\phi_0 = 4.1125, \rho_0 \approx 0.38$. To Validate the correctness of the acquired assertions of Theorem 3.1, we select two different delay numbers. One is $\rho = 0.2$ and one is $\rho = 0.45$. For $\rho = 0.2 < \rho_0 \approx 0.38$, we acquire Matlab simulation plots which are provided in Figures 1-4. In view of Figures 1-4, one can lightly know that $u_1 \to 5, u_2 \to 26$ when $t \to +\infty$. That is to say, the equilibrium point $E(5, 26)$ of system (71) remains locally asymptotically stable level. For $\rho = 0.45 > \rho_0 \approx 0.38$, we acquire Matlab simulation plots which are provided in Figures 5-8. In view of Figures 5-8, one can lightly know that u_1 is about to remain periodic oscillation near the number 5, u_2 is about to remain periodic oscillation near the number 26. Namely, a family of limit cycles (i.e., Hopf bifurcations) take place around the equilibrium point $E(5, 26)$. Besides, the bifurcation diagrams, which distinctly show

the bifurcation point of system (71), are given in Figures 9-10. In view of Figures 9-10, one can lightly know that the bifurcation value of system (71) is $\rho_0 \approx 0.38$.

Example 6.2. Consider the following controlled chlorine dioxide-iodine-malonic acid chemical reaction model incorporating delays:

$$\begin{cases} \dfrac{du_1(t)}{dt} = 0.25\left[1 - u_1(t) - \dfrac{4u_1(t)u_2(t)}{1+u_1^2(t-\rho)}\right] \\ \qquad\qquad - 0.8[u_1(t-\rho) - u_1(t)], \\ \dfrac{du_2(t)}{dt} = 10u_1(t)\left[1 - \dfrac{u_2(t)}{1+u_1^2(t-\rho)}\right]. \end{cases} \tag{72}$$

Obviously, system (72) owns a unique positive equilibrium point $E(5, 26)$. We can lightly check that the assumptions $(\mathcal{G}_4)$-$(\mathcal{G}_6)$ of Theorem 4.1 are satisfied. Taking advantage of Matlab software, we can gain that $\omega_0 = 2.5622, \rho_{0\star} \approx 0.46$. To Validate the correctness of the acquired assertions of Theorem 4.1, we select two different delay numbers. One is $\rho = 0.45$ and one is $\rho = 0.498$. For $\rho = 0.45 < \rho_{0\star} \approx 0.46$, we acquire Matlab simulation plots which are provided in Figures 11-14. In view of Figures 11-14, one can lightly know that $u_1 \to 5, u_2 \to 26$ when $t \to +\infty$. That is to say, the equilibrium point $E(5, 26)$ of system (72) keeps locally asymptotically stable level. For $\rho = 0.498 > \rho_{0\star} \approx 0.46$, we acquire Matlab simulation plots which are provided in Figures 15-18. In view of Figures 15-18, one can lightly know that u_1 is about to remain periodic oscillation near the number 5, u_2 is about to remain periodic oscillation near the number 26. Namely, a family of limit cycles (i.e., Hopf bifurcations) take place around the equilibrium point $E(5, 26)$. Besides, the bifurcation diagrams, which distinctly show the bifurcation point of system (72), are given in Figures 19-20. In view of Figures 19-20, one can lightly know that the bifurcation value of system (72) is $\rho_{0\star} \approx 0.46$.

Example 6.3. Consider the following controlled chlorine dioxide-iodine-

malonic acid chemical reaction model incorporating delays:

$$\begin{cases} \dfrac{du_1(t)}{dt} = 0.5 \times 0.25 \left[1 - u_1(t) - \dfrac{4u_1(t)u_2(t)}{1 + u_1^2(t-\rho)}\right] \\ \qquad\qquad - 0.5[u_1(t) - u_{1\star}], \\ \dfrac{du_2(t)}{dt} = 10u_1(t) \left[1 - \dfrac{u_2(t)}{1 + u_1^2(t-\rho)}\right]. \end{cases} \tag{73}$$

Obviously, system (73) owns a unique positive equilibrium point $E(5, 26)$. We can lightly check that the assumptions $(\mathcal{G}_7)$-$(\mathcal{G}_9)$ of Theorem 5.1 are satisfied. Taking advantage of Matlab software, we can gain that $\varpi_0 = 5.0067, \rho_{0\diamond} \approx 0.18$. To Validate the correctness of the acquired assertions of Theorem 5.1, we select two different delay numbers. One is $\rho = 0.02$ and one is $\rho = 0.23$. For $\rho = 0.02 < \rho_{0\diamond} \approx 0.18$, we acquire Matlab simulation plots which are provided in Figures 21-24. In view of Figures 21-24, one can lightly know that $u_1 \to 5, u_2 \to 26$ when $t \to +\infty$. That is to say, the equilibrium point $E(5, 26)$ of system (73) keeps locally asymptotically stable level. For $\rho = 0.23 > \rho_{0\diamond} \approx 0.18$, we acquire Matlab simulation plots which are provided in Figures 25-28. In view of Figures 25-28, one can lightly know that u_1 is about to remain periodic oscillation near the number 5, u_2 is about to remain periodic oscillation near the number 26. Namely, a family of limit cycles (i.e., Hopf bifurcations) take place around the equilibrium point $E(5, 26)$. Besides, the bifurcation diagrams, which distinctly show the bifurcation point of system (73), are given in Figures 29-30. In view of Figures 29-30, one can lightly know that the bifurcation value of system (73) is $\rho_{0\diamond} \approx 0.18$.

Remark 6.1. *In system (71), we gain the bifurcation value $\rho_0 \approx 0.38$. In system (72), we gain bifurcation value $\rho_{0\star} \approx 0.46$. In system (73), we gain bifurcation value $\rho_{0\diamond} \approx 0.18$. We can easily see that the stability region of system (71) is enlarged and the time of generation of Hopf bifurcation of system (71) is delayed by virtue of hybrid controller I consisting of state feedback and parameter perturbation with delay and the stability region of system (71) is narrowed and the time of generation of Hopf bifurcation of system (71) is advanced by virtue of hybrid controller II consisting of state feedback and parameter perturbation without delay.*

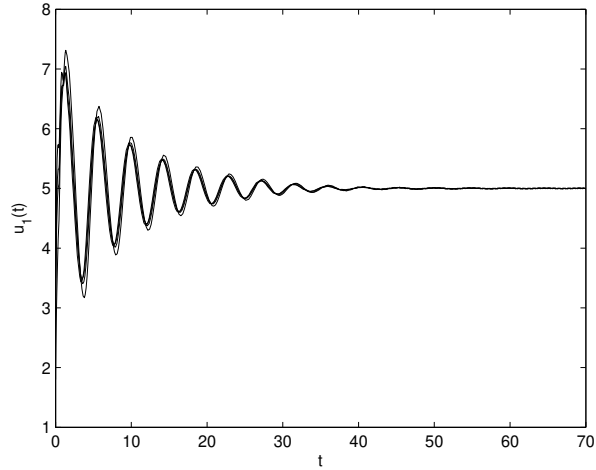

Figure 1. Matlab simulation plots of system (71) under the condition $\rho = 0.2 < \rho_0 \approx 0.38$. The relation of t and $u_1(t)$. The positive equilibrium point $E(5, 26)$ maintains locally asymptotically stable level.

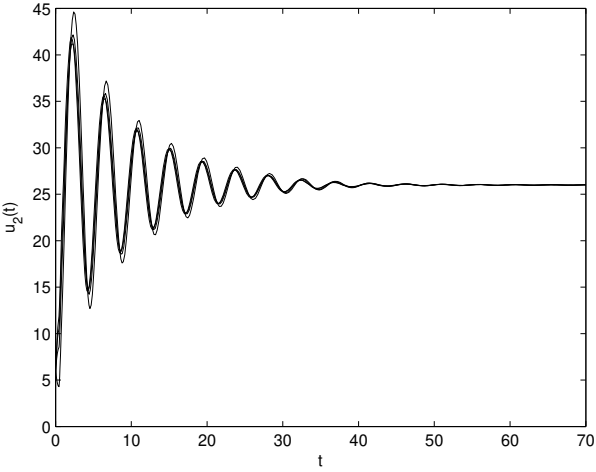

Figure 2. Matlab simulation plots of system (71) under the condition $\rho = 0.2 < \rho_0 \approx 0.38$. The relation of t and $u_2(t)$. The positive equilibrium point $E(5, 26)$ maintains locally asymptotically stable level.

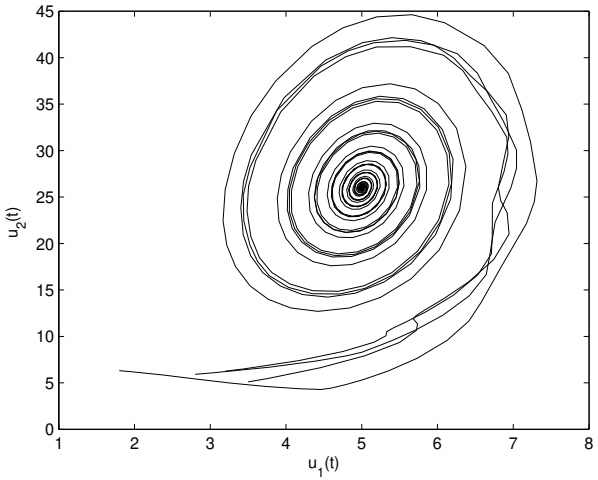

Figure 3. Matlab simulation plots of system (71) under the condition $\rho = 0.2 < \rho_0 \approx 0.38$. The relation of $u_1(t)$ and $u_2(t)$. The positive equilibrium point $E(5, 26)$ maintains locally asymptotically stable level.

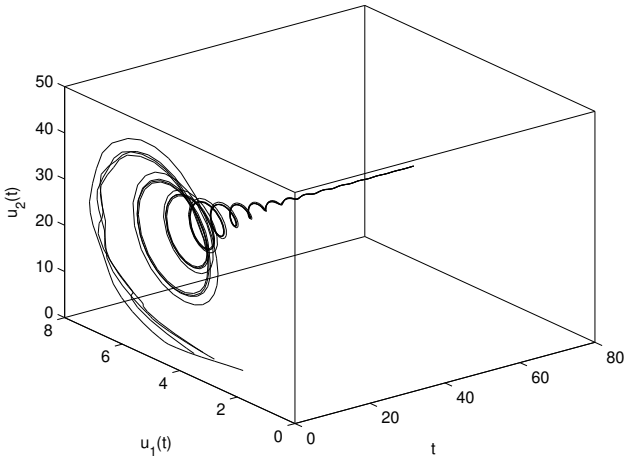

Figure 4. Matlab simulation plots of system (71) under the condition $\rho = 0.2 < \rho_0 \approx 0.38$. The relation of t, $u_1(t)$ and $u_2(t)$. The positive equilibrium point $E(5, 26)$ maintains locally asymptotically stable level.

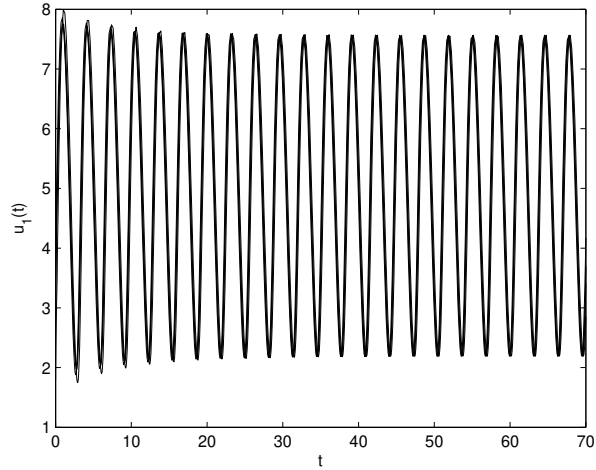

Figure 5. Matlab simulation plots of system (71) under the condition $\rho = 0.45 > \rho_0 \approx 0.38$. The relation of t and $u_1(t)$. A family of limit cycles (i.e., Hopf bifurcations) take place around the positive equilibrium point $E(5, 26)$.

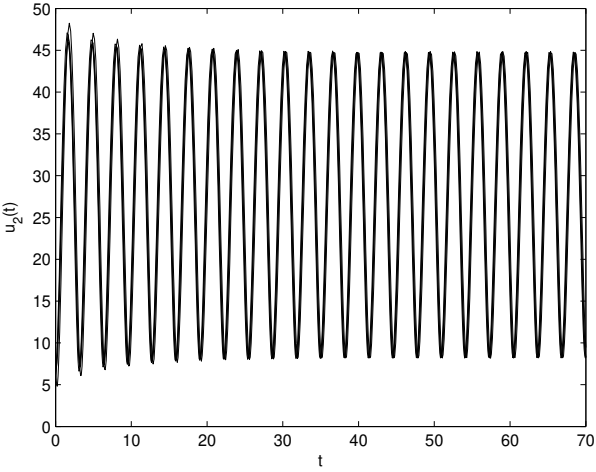

Figure 6. Matlab simulation plots of system (71) under the condition $\rho = 0.45 > \rho_0 \approx 0.38$. The relation of t and $u_2(t)$. A family of limit cycles (i.e., Hopf bifurcations) take place around the positive equilibrium point $E(5, 26)$.

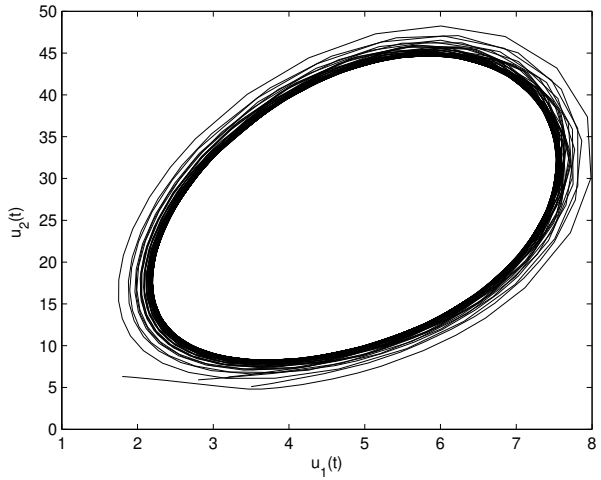

Figure 7. Matlab simulation plots of system (71) under the condition $\rho = 0.45 > \rho_0 \approx 0.38$. The relation of $u_1(t)$ and $u_1(t)$. A family of limit cycles (i.e., Hopf bifurcations) take place around the positive equilibrium point $E(5, 26)$.

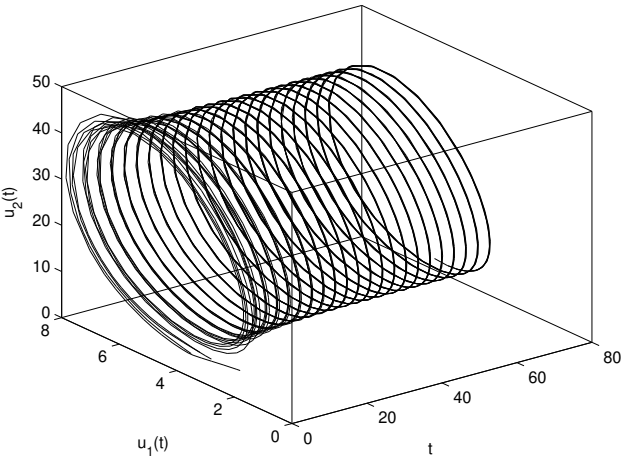

Figure 8. Matlab simulation plots of system (71) under the condition $\rho = 0.45 > \rho_0 \approx 0.38$. The relation of t, $u_1(t)$ and $u_2(t)$. A family of limit cycles (i.e., Hopf bifurcations) take place around the positive equilibrium point $E(5, 26)$.

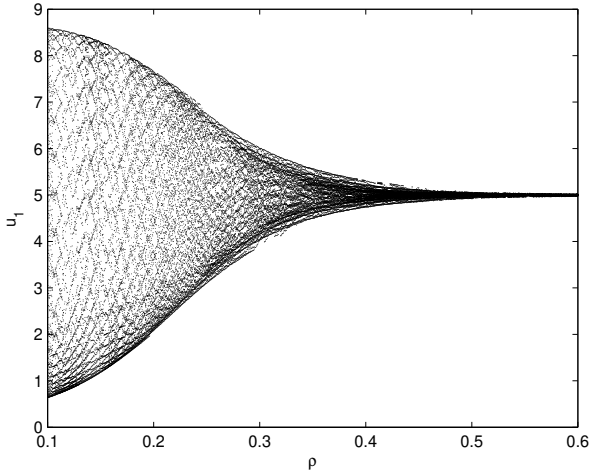

Figure 9. Bifurcation diagram of system (71): the time variable t versus the state variable u_1. The bifurcation value $\rho_0 \approx 0.38$.

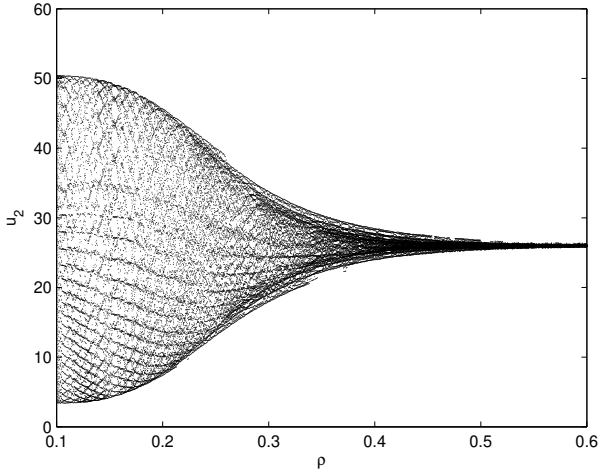

Figure 10. Bifurcation diagram of system (71): the time variable t versus the state variable u_2. The bifurcation value $\rho_0 \approx 0.38$.

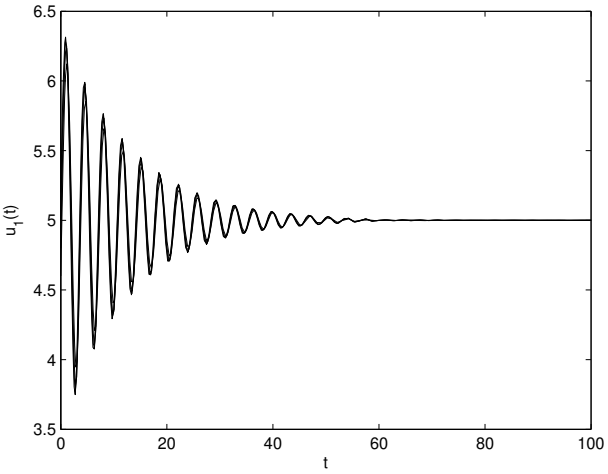

Figure 11. Matlab simulation plots of system (72) under the condition $\rho = 0.45 < \rho_{0\star} \approx 0.46$. The relation of t and $u_1(t)$. The positive equilibrium point $E(5, 26)$ maintains locally asymptotically stable level.

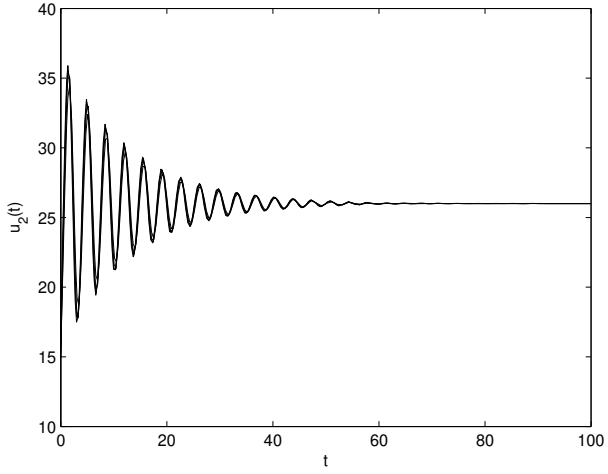

Figure 12. Matlab simulation plots of system (72) under the condition $\rho = 0.45 < \rho_{0\star} \approx 0.46$. The relation of t and $u_2(t)$. The positive equilibrium point $E(5, 26)$ maintains locally asymptotically stable level.

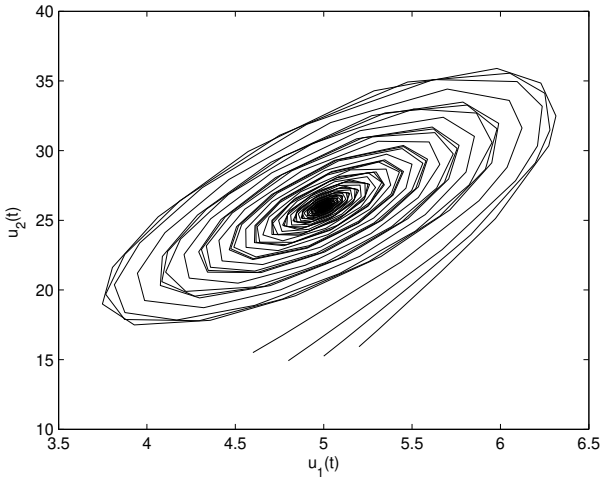

Figure 13. Matlab simulation plots of system (72) under the condition $\rho = 0.45 < \rho_{0\star} \approx 0.46$. The relation of $u_1(t)$ and $u_2(t)$. The positive equilibrium point $E(5, 26)$ maintains locally asymptotically stable level.

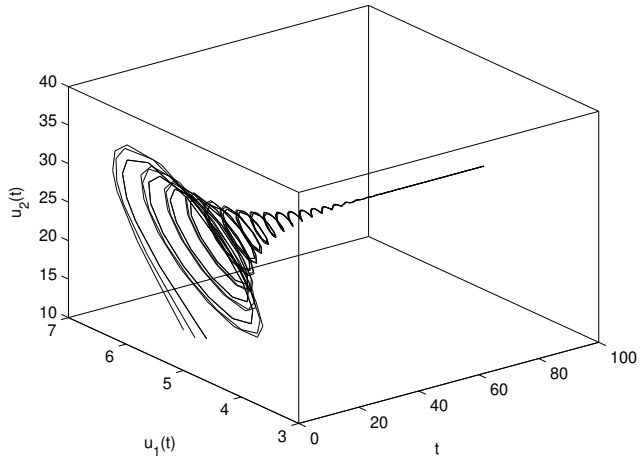

Figure 14. Matlab simulation plots of system (72) under the condition $\rho = 0.45 < \rho_{0\star} \approx 0.46$. The relation of t, $u_1(t)$ and $u_2(t)$. The positive equilibrium point $E(5, 26)$ maintains locally asymptotically stable level.

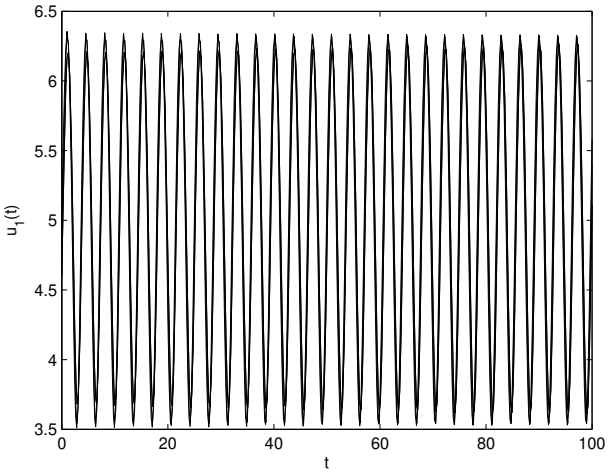

Figure 15. Matlab simulation plots of system (72) under the condition $\rho = 0.498 > \rho_{0\star} \approx 0.46$. The relation of t and $u_1(t)$. A family of limit cycles (i.e., Hopf bifurcations) take place around the positive equilibrium point $E(5, 26)$.

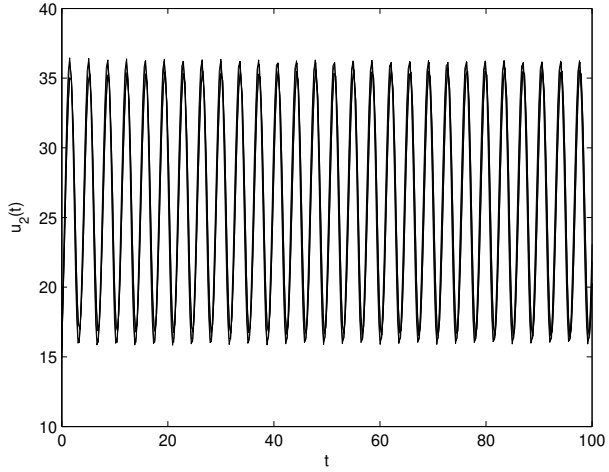

Figure 16. Matlab simulation plots of system (72) under the condition $\rho = 0.498 > \rho_{0\star} \approx 0.46$. The relation of t and $u_2(t)$. A family of limit cycles (i.e., Hopf bifurcations) take place around the positive equilibrium point $E(5, 26)$.

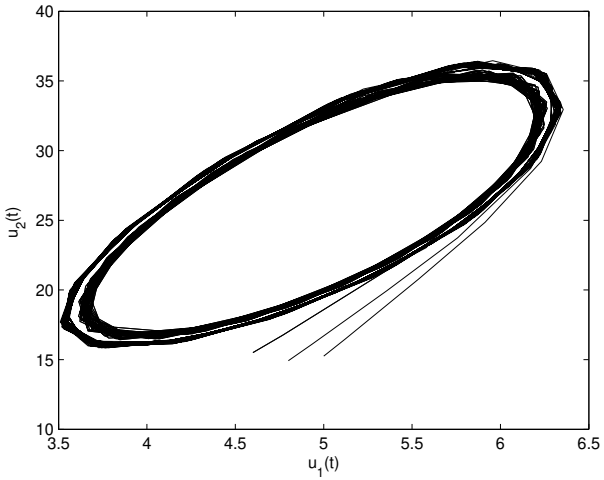

Figure 17. Matlab simulation plots of system (72) under the condition $\rho = 0.498 > \rho_{0\star} \approx 0.46$. The relation of $u_1(t)$ and $u_1(t)$. A family of limit cycles (i.e., Hopf bifurcations) take place around the positive equilibrium point $E(5, 26)$.

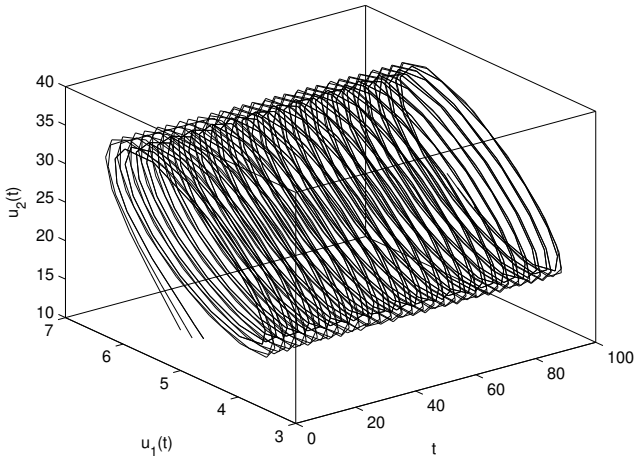

Figure 18. Matlab simulation plots of system (72) under the condition $\rho = 0.498 > \rho_{0\star} \approx 0.46$. The relation of t, $u_1(t)$ and $u_1(t)$. A family of limit cycles (i.e., Hopf bifurcations) take place around the positive equilibrium point $E(5, 26)$.

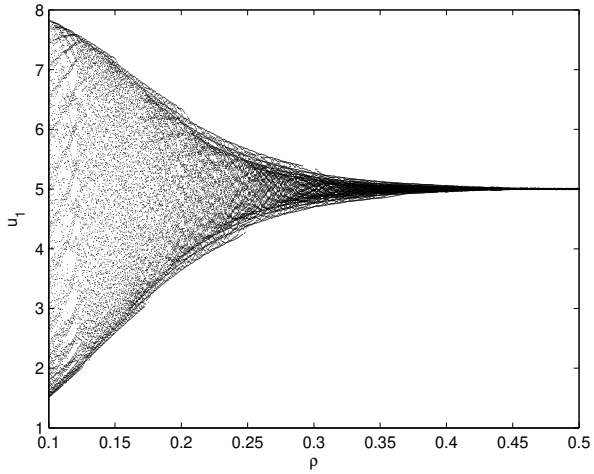

Figure 19. Bifurcation diagram of system (72): the time variable t versus the state variable u_1. The bifurcation value $\rho_{0\star} \approx 0.46$.

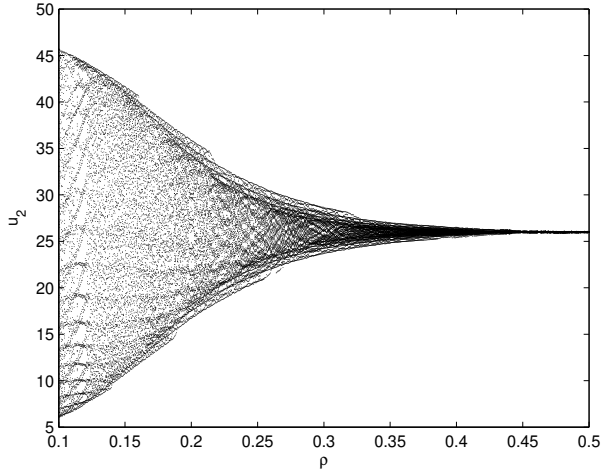

Figure 20. Bifurcation diagram of system (72): the time variable t versus the state variable u_2. The bifurcation value $\rho_{0\star} \approx 0.46$.

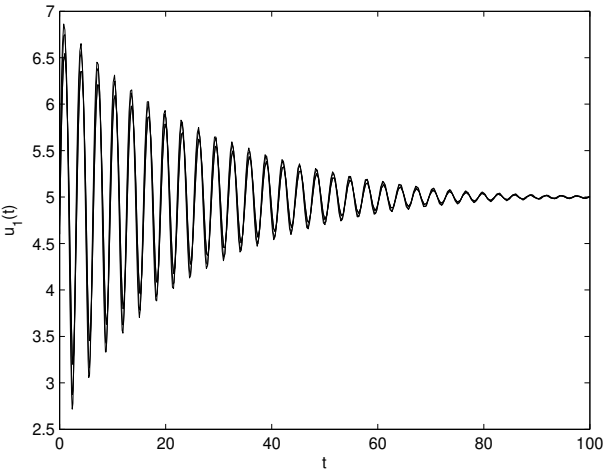

Figure 21. Matlab simulation plots of system (73) under the condition $\rho = 0.02 < \rho_{0\diamond} \approx 0.18$. The relation of t and $u_1(t)$. The positive equilibrium point $E(5, 26)$ maintains locally asymptotically stable level.

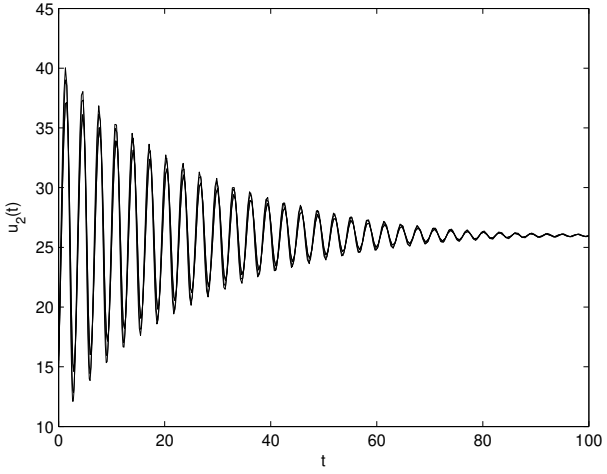

Figure 22. Matlab simulation plots of system (73) under the condition $\rho = 0.02 < \rho_{0\diamond} \approx 0.18$. The relation of t and $u_2(t)$. The positive equilibrium point $E(5, 26)$ maintains locally asymptotically stable level.

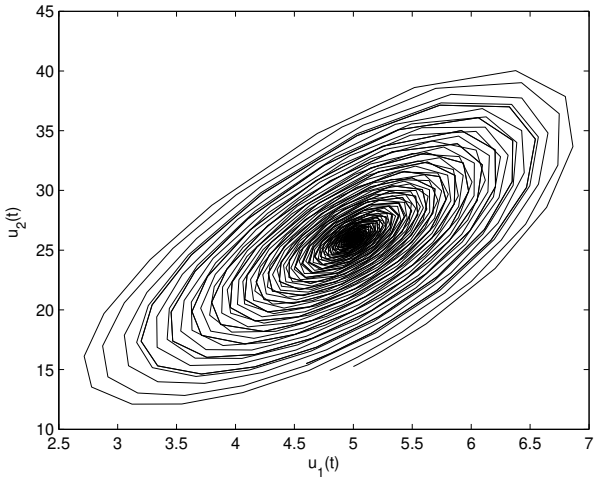

Figure 23. Matlab simulation plots of system (73) under the condition $\rho = 0.02 < \rho_{0\diamond} \approx 0.18$. The relation of $u_1(t)$ and $u_2(t)$. The positive equilibrium point $E(5, 26)$ maintains locally asymptotically stable level.

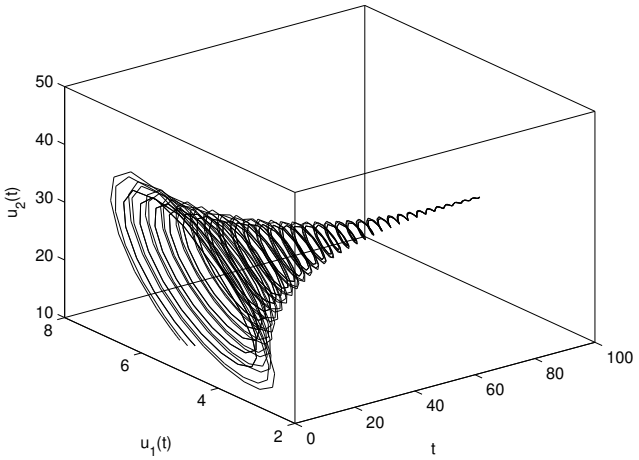

Figure 24. Matlab simulation plots of system (73) under the condition $\rho = 0.02 < \rho_{0\diamond} \approx 0.18$. The relation of t, $u_1(t)$ and $u_2(t)$. The positive equilibrium point $E(5, 26)$ maintains locally asymptotically stable level.

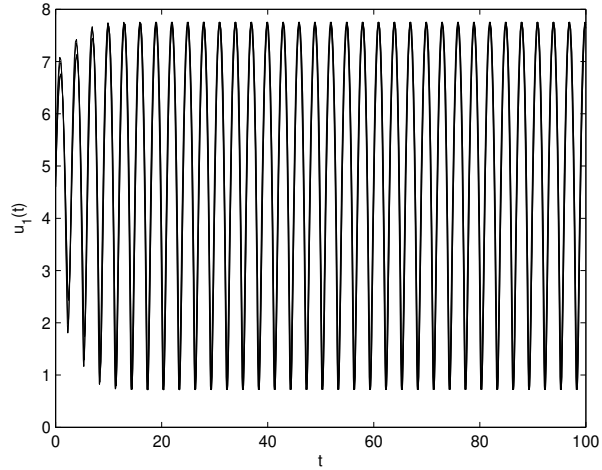

Figure 25. Matlab simulation plots of system (73) under the condition $\rho = 0.23 > \rho_{0\diamond} \approx 0.18$. The relation of t and $u_1(t)$. A family of limit cycles (i.e., Hopf bifurcations) take place around the positive equilibrium point $E(5, 26)$.

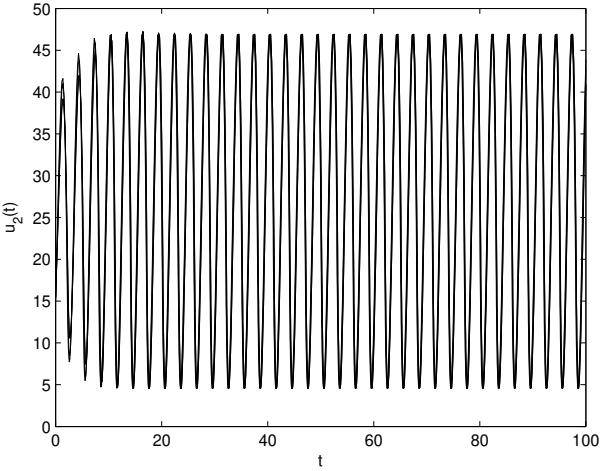

Figure 26. Matlab simulation plots of system (73) under the condition $\rho = 0.23 > \rho_{0\diamond} \approx 0.18$. The relation of t and $u_2(t)$. A family of limit cycles (i.e., Hopf bifurcations) take place around the positive equilibrium point $E(5, 26)$.

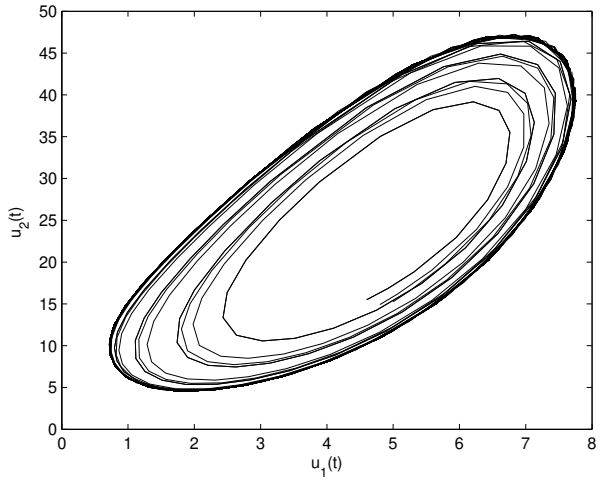

Figure 27. Matlab simulation plots of system (73) under the condition $\rho = 0.23 > \rho_{0\diamond} \approx 0.18$. The relation of $u_1(t)$ and $u_1(t)$. A family of limit cycles (i.e., Hopf bifurcations) take place around the positive equilibrium point $E(5, 26)$.

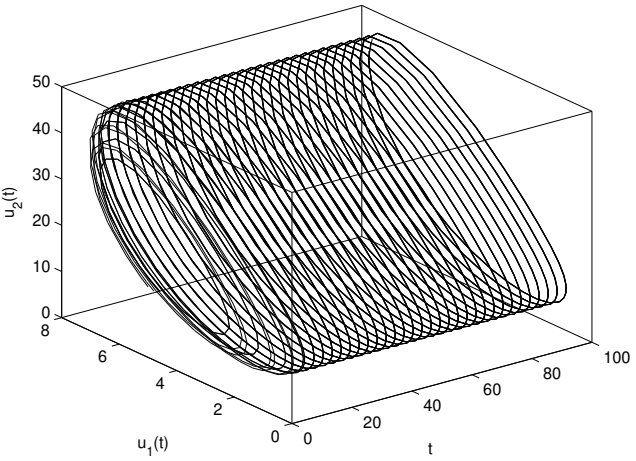

Figure 28. Matlab simulation plots of system (73) under the condition $\rho = 0.23 > \rho_{0\diamond} \approx 0.18$. The relation of t, $u_1(t)$ and $u_1(t)$. A family of limit cycles (i.e., Hopf bifurcations) take place around the positive equilibrium point $E(5, 26)$.

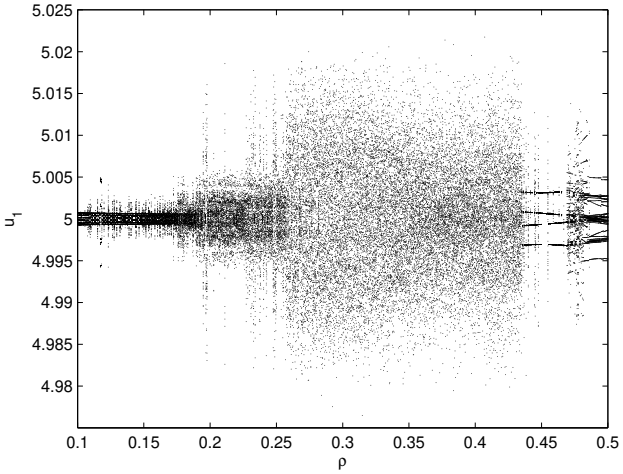

Figure 29. Bifurcation diagram of system (73): the time variable t versus the state variable u_1. The bifurcation value $\rho_{0\diamond} \approx 0.18$.

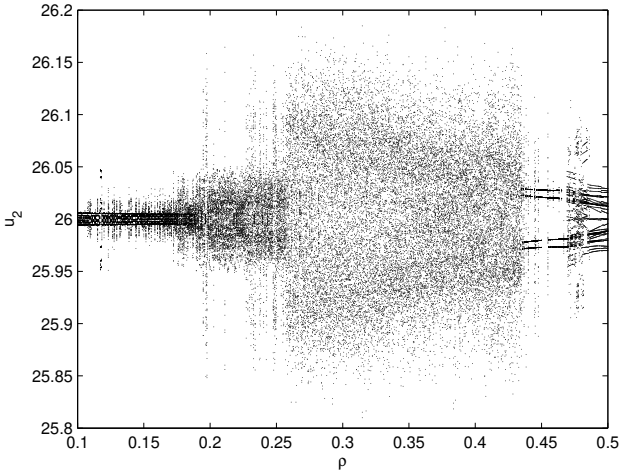

Figure 30. Bifurcation diagram of system (73): the time variable t versus the state variable u_2. The bifurcation value $\rho_{0\diamond} \approx 0.18$.

7 Conclusions

At present, the exploration on chemical reaction model has aroused great interest from chemical and mathematical circles. Mathematically speaking, uncovering the influence of delay on the various dynamical behavior of chemical reaction models is an important theme. In this present research, a novel chlorine dioxide-iodine-malonic acid chemical reaction model incorporating delays is established. The existence and uniqueness, non-negativeness of solution to the formulated delayed chlorine dioxide-iodine-malonic acid chemical reaction model are investigated in detail. By regarding the delay as bifurcation parameter, we acquire a delay-independent criterion ensuring the stability and generation of bifurcation of the formulated delayed chlorine dioxide-iodine-malonic acid chemical reaction model. By virtue of two reasonable hybrid controllers containing state feedback and parameter perturbation, we can successfully dominate the stability domain and the time of generation of Hopf bifurcation of the formulated delayed chlorine dioxide-iodine-malonic acid chemical reaction model. The acquired outcomes of this research possess momentous theoretical value in preserving the balance of the concentrations of chlorine dioxide, iodine in chemistry. What is more, the research way can be helpful in exploring the bifurcation control question of abundant other dynamical models.

***Acknowledgment*:** This work is supported by National Natural Science Foundation of China (No.12261015, No.62062018), Project of High-level Innovative Talents of Guizhou Province ([2016]5651), University Science and Technology Top Talents Project of Guizhou Province (KY[2018]047), Foundation of Science and Technology of Guizhou Province ([2019]1051), Guizhou University of Finance and Economics(2018XZD01), Guizhou University of Finance and Economics Project Funding (No.2019XYB11), Guizhou Science and Technology Platform Talents ([2017] 5736-019). The authors would like to thank the referees and the editor for helpful suggestions incorporated into this paper.

References

[1] B. P. Belousov, *A Periodic Reaction and Its Mechanism*, Wiley, New York, 1985, pp. 605–605.

[2] A. M. Zhabotinskii, Periodic process of the oxidation of malonic acid in solution (Study of the kinetics of Belousov's), *Biofizika* **9** (1964) 306–311.

[3] Q. Din, T. Donchev, D. Kolev, Stability, Bifurcation analysis and chaos control in chlorine dioxide-iodine-malonic acid reaction, *MATCH Commun. Math. Comput. Chem.* **79** (2018) 577–606.

[4] I. Lengyel, G. Ribai, I. R. Epstein, Experimental and modeling study of oscillations in the chlorine dioxide-iodine-malonic acid reaction, *J. Am. Chem. Soc.* **112** (1990) 9104–9110.

[5] E. Mosekilde, *Topics in Nonlinear Dynamics: Applications to Physics, Biology and Economic Systems*, World Sci. Publ., New Jersey, 1996.

[6] J. N. Wang, H. B. Shi, L. Xu, L. Zang, Hopf bifurcation and chaos of tumor-Lymphatic model with two time delays, *Chaos Solitons Fractals* **157** (2022) #111922.

[7] N. C. Pati, B. Ghosh, Delayed carrying capacity induced subcritical and supercritical Hopf bifurcations in a predator–prey system, *Math. Comput. Simul.* **195** (2022) 171–196.

[8] C. J. Xu, Z. X. Liu, M. X. Liao, L. Y. Yao, Theoretical analysis and computer simulations of a fractional order bank data model incorporating two unequal time delays, *Expert Syst. Appl.* **199** (2022) #116859.

[9] C. J. Xu, W. Zhang, C. Aouiti, Z. X. Liu, L. Y. Yao, Further analysis on dynamical properties of fractional-order bi-directional associative memory neural networks involving double delays, *Math. Meth. Appl. Sci.* (2022) doi: 10.1002/mma.8477

[10] C. J. Xu, M. X. Liao, P. L. Li, Y. Guo, Z. X. Liu, Bifurcation properties for fractional order delayed BAM neural networks, *Cogn. Comput.* **13** (2021) 322–356.

[11] C. J. Xu, W. Zhang, Z. X. Liu, L. Y. Yao, Delay-induced periodic oscillation for fractional-order neural networks with mixed delays, *Neurocomput.* **488** (2022) 681–693.

[12] C. J. Xu, D. Mu, Z. X. Liu, Y. C. Pang, M. X. Liao, P. Li, Bifurcation dynamics and control mechanism of a fractional-order delayed Brusselator chemical reaction model, *MATCH Commun. Math. Comput. Chem.* **89** (2023) 73–106.

[13] C. J. Xu, C. Aouiti, Z. X. Liu, P. L. Li, L. Y. Yao, Bifurcation caused by delay in a fractional-order coupled Oregonator model in chemistry, *MATCH Commun. Math. Comput. Chem.* **88** (2022) 371–396.

[14] C. J. Xu, W. Zhang, C. Aouiti, Z. X. Liu, P. L. Li, Bifurcation dynamics in a fractional-order Oregonator model including time delay, *MATCH Commun. Math. Comput. Chem.* **87** (2022) 397–414.

[15] C. J. Xu, D. Mu, Z. X. Liu, Y. C. Pang, M. X. Liao, P. L. Li, Bifurcation dynamics and control mechanism of a fractional-order delayed Brusselator chemical reaction model, *MATCH Commun. Math. Comput. Chem.* **89** (2023) 73–106.

[16] C. R. Tian, Y. Liu, Delay-driven Hopf bifurcation in a networked Malaria model, *Appl. Math. Lett.* **132** (2022) #108092.

[17] H. L. Li, L. Zhang, C. Hu, Y. L. Jiang, Z. D. Teng, Dynamical analysis of a fractional-order prey-predator model incorporating a prey refuge, *J. Appl. Math. Comput.* **54** (2017) 435–449.

[18] M. Das, A. Maiti, G.P. Samanta, Stability analysis of a prey-predator fractional order model incorporating prey refuge, *Ecol. Genet. Genom.* **7-8** (2018) 33–46.

[19] Z. Z. Zhang, H. Z. Yang, *Hybrid control of Hopf bifurcation in a two prey one predator system with time delay*, Proceed, 33rd Chinese Control Conference, Nanjing, China, July 28-30 (2014) 6895–6900.

[20] L. P. Zhang, H. N. Wang, M. Xu, Hybrid control of bifurcation in a predator-prey system with three delays, *Acta Phys. Sinica* **60** (2011) #010506.

[21] Z. Liu, K.W. Chuang, Hybrid control of bifurcation in continuous nonlinear dynamical systems, *Int. J. Bifur. Chaos* **15** (2005) 1895–3903.